doi:10.1246/cl.2010.64

Published on the web December 12, 2009

Fabrication of Ni/Al_2O_3 Core–Shell Nanowire Arrays in Porous Alumina Membranes

Chengyong Li, Xuehua Wang,* Gui Chen, Lei He, and Hong Cao
School of Materials Science and Engineering, Wuhan Institute of Technology, Wuhan 430073, P. R. China

(Received September 3, 2009; CL-090806)

Ordered Ni/Al_2O_3 core–shell nanowire arrays were prepared in porous alumina membrane via alternating current electrodeposition and chemical etching methods. The shape of the inner Ni core is columnar with a diameter of 50 nm. The shape of the outer Al_2O_3 shell is a regular hexagon and the well thickness is about 40 nm. This novel structured material can be used as a media for magnetic storage and high-temperature nanoelectronic devices.

Ni nanostructured materials have attracted great attention over the past decade because of their potential use in high density perpendicular magnetic memories,[1] high sensitivity magnetic sensors,[2] catalysts,[3] hydrogen storage materials,[4] and other applications.[5] Ni nanopowders have been used in catalysts[6] and coating materials[7] in the early years. Recently, it was discovered that characteristic parameters of nanostructured materials have a strong relation to morphology.[8] In particular, the application of Ni has been further expanded due to the successful preparation of one-dimensional Ni nanostructure materials. Magnetic memories of Ni nanowire arrays have been extensively studied in recent years.[9] But the applications of nanowires have been limited because nanowires are subject to oxidation under service due to their small size and huge specific surface area. In order to overcome these shortages, it is necessary to cover the surface of the Ni nanowires with another material.

In this letter, we report an easy route to fabricate Ni/Al_2O_3 core–shell nanowire arrays. The Ni core can maintain high activity and avoid oxidization because of the outer cover layer. Meanwhile, this new nanostructured material may have potential applications in magnetic storage and high-temperature nanoelectronic devices due to its high thermal and chemical stability[10] and important dielectric properties[11] of alumina. The morphology of Ni/Al_2O_3 core–shell nanowire arrays were studied by field emission scanning electron microscopy (FE-SEM, model Sirion 200). Furthermore, the formation mechanism of the Ni/Al_2O_3 core–shell nanostructure is also discussed.

The fabrication of Ni/Al_2O_3 core–shell nanowire arrays is shown in Figure 1. First, a two-step anodic oxidation technique, which has been described in ref 12, was applied to prepare the porous alumina membrane (PAM). The anodization was carried out in 0.4 mol L^{-1} oxalic acid solution at 50 V_{DC} and 20 °C. The duration of the first step anodization was 0.5 h, and that of the second step anodization was 4 h. After anodization, a technique of reducing the anodization voltage from 50 to 10 V_{DC} at 1 V min^{-1}, as described in ref 13, was applied to thin the barrier layer in order to increase the deposition rate during the alternating current (AC) electrodeposition.

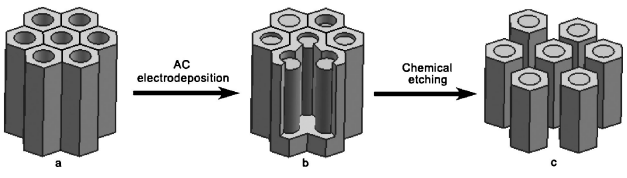

Figure 1. Fabrication of Ni/Al_2O_3 core–shell nanowire arrays: (a) PAM with highly ordered nanopores, (b) filling of Ni nanowires into alumina pores via AC electrodeposition, and (c) Ni/Al_2O_3 core–shell nanowire arrays.

The main electrolytic solution had the following fixed composition as described in Table 1. Nickel sulfate was the source for metal ions, ascorbic acid was used as a complexing agent, and boric acid acted as a buffering agent to control pH of the electrolyte during the deposition process. All chemicals were analytical reagent grade. After deposition, the sample was washed thoroughly with distilled water several times and flooded by heated N_2 flow for 10 min. Then the sample was immersed in 1 mol L^{-1} NaOH solution and subjected to ultrasonic treatment for 20 min at 20 °C.

Figure 2 shows a SEM image of the surface view of the PAM after the second anodization at 50 V_{DC} in 0.4 mol L^{-1} oxalic acid solution at 20 °C. A well-ordered array and honeycomb texture of nanopores is observed. The pore channels are parallel to and lie perpendicular to the surface of the membrane. The diameter of the pores is on the order of 50 nm, and pore density can be as high as 1.0×10^{10} cm^{-2}.

Figure 3 shows a SEM image of the Ni/Al_2O_3 core–shell nanowire arrays and diameter distribution diagrams of the cores and shells. The remarkable feature of this nanostructure is that the shape of the inner Ni cores is columnar and that of the outer Al_2O_3 shell is a regular hexagon. Meanwhile, almost every nanowire is parallel. The inset of Figure 3 clearly shows a magnified SEM image of Ni/Al_2O_3 core–shell nanowire. The diameter of the inner Ni core and the outer Al_2O_3 shell were about 52 and 130 nm, respectively. The diameters of Ni core and Al_2O_3 shell are in accordance with the pore size and cell size of the PAM, respectively. The whole shape of the Ni/Al_2O_3 core–shell nanowires is the same as the regular hexagonal cell structure of the back of the PAM as shown in Figure 4. From the Figures 3a and 3b, we know that the core–shell structure has good uniformity in diameter. But we find that the height of Ni/Al_2O_3 core–shell nanowires is slightly nonuniform and is not the same as the thickness of porous layer of the PAM, which would be caused by the nonuniformity of length of Ni nanowires

Table 1. Composition and operating parameters of AC electrodeposition for Ni

Composition/operation parameters	Specification
$NiSO_4 \cdot 6H_2O$/g L^{-1}	60
H_3BO_3/g L^{-1}	30
Ascorbic acid/g L^{-1}	5
Voltage/V	10
Frequency/Hz	50
Time/min	90
pH	3.5
Temperature/°C	20

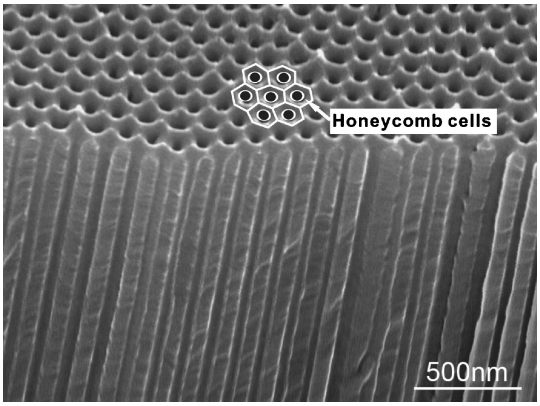

Figure 2. SEM image of PAM anodized at 50 V_{DC} in 0.4 mol L^{-1} $H_2C_2O_4$.

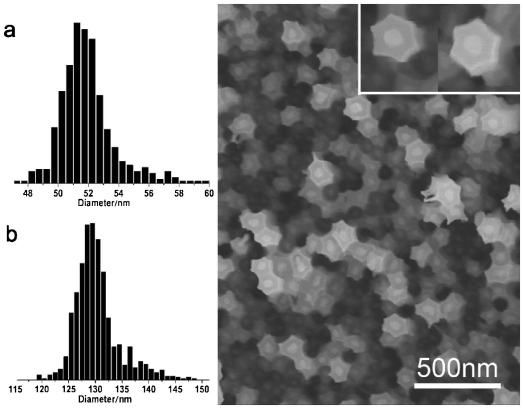

Figure 3. SEM image of Ni/Al_2O_3 core–shell nanowire arrays (a. diameter distribution diagram of Ni cores and b. diameter distribution diagram of Al_2O_3 shells).

deposited via the AC electrodeposition as shown in Figure 1. Such nonuniformity can be eliminated by increasing deposition time appropriately during AC electrodeposition.

Figure 4 shows a two-dimensional honeycomb cell of the back of the PAM. Apparently, each cell has a regular hexagonal structure and the cell arrangement is highly ordered. In the previous literature, some authors have proposed that the voids are located at triple points between cell grains in the PAM.[14] We propose a probable formation mechanism of Ni/Al_2O_3 core–shell nanowire arrays on the basis of previous theory, which may be explained as follows: there are many voids in the cell boundaries; the plane where voids locate is weak; the breaking spots of the cells locate at this plane; the cells break down from the apex where the stress concentration point is and which has higher chemical activity, as shown in Figure 5. When ultrasonic treatment is applied to the PAM, the tensile stress changes abruptly and promotes microcrack initiation from the apex. Meanwhile, microcracks propagate along the weak plane due to stress and chemical etching by NaOH solution. As time passes, microcracks can split the junctions between the voids and thus lead to the interlaced cleavage of the cells. As a result, each cell will separate from each other to form Ni/Al_2O_3 core–shell nanowire.

In conclusion, ordered Ni/Al_2O_3 core–shell nanowire arrays were successfully fabricated in PAM using AC electrodeposition

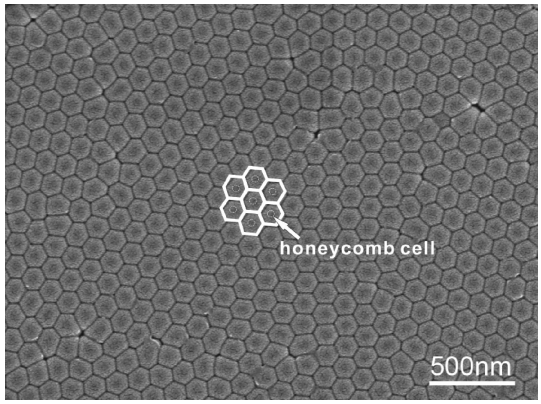

Figure 4. SEM image of the back of the PAM.

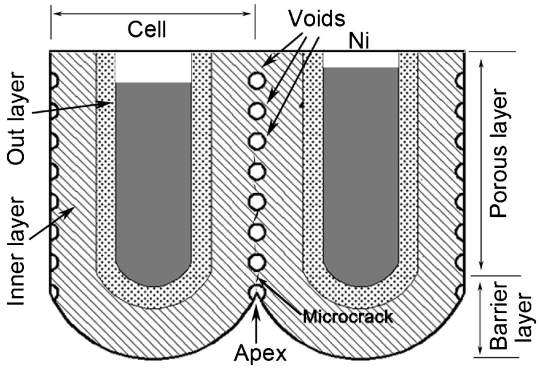

Figure 5. Schematic diagram of porous alumina oxide layers consisting of voids between two outer layers and apex point of microcrack initiation.

and chemical etching methods. This new structure material obtained by the present process can be used for the preparation of various types of magnetic storage and high-temperature nanoelectronic devices.

This work was supported by the Wuhan Chenguang Plan Foundation in Hubei Prov., P. R. China through Grant No. 20065004116-35 to one of the authors (Xuehua Wang). The provided supports are gratefully acknowledged.

References

1 a) S.-Z. Chu, K. Wada, S. Inoue, S. Todoroki, *Chem. Mater.* **2002**, *14*, 4595. b) F. Tian, J. Zhu, D. Wei, *J. Phys. Chem. C* **2007**, *111*, 6994. c) W. J. Zheng, G. T. Fei, B. Wang, L. D. Zhang, *Chem. Lett.* **2009**, *38*, 394.
2 a) P. Granitzer, K. Rumpf, H. Krenn, *Mater. Res. Soc. Symp. Proc.* **2005**, *876E*, R8.9.1. b) Z. K. Bai, C. S. Xie, M. L. Hu, S. P. Zhang, *Physica E* **2008**, *41*, 235.
3 E. G. Wang, *J. Mater. Res.* **2006**, *21*, 2767.
4 J. P. Li, X. F. Ji, F. Wu, G. Q. Wang, *Adv. Mater.* **1993**, *5*, 554.
5 R.-M. Liu, J.-M. Ting, J.-C. A. Huang, C.-P. Liu, *Thin Solid Films* **2002**, *420–421*, 145.
6 D. H. Zuo, Z. K. Zhang, Z. L. Cui, *J. Mol. Catal.* **1995**, *9*, 298.
7 Y. T. Pei, J. H. Ouyang, T. C. Lei, Y. Zhou, *Mater. Sci. Eng., A* **1995**, *194*, 219.
8 J. Ma, H. Liu, Y. Shi, J. He, Z. K. Yao, *Chin. J. Appl. Chem.* **2008**, *25*, 815.
9 D. Navas, K. R. Pirota, P. Mendoza Zelis, D. Velazquez, C. A. Ross, M. Vazquez, *J. Appl. Phys.* **2008**, *103*, 07D523.
10 G. Das, *Ceram. Eng. Sci. Proc.* **1995**, *16*, 977.
11 Y. C. Wang, I. C. Leu, M. H. Hon, *J. Appl. Phys.* **2004**, *95*, 1444.
12 H. Masuda, K. Fukuda, *Science* **1995**, *268*, 1466.
13 R. C. Furneaux, W. R. Rigby, A. P. Davidson, *Nature* **1989**, *337*, 147.
14 D. D. Macdonald, *J. Electrochem. Soc.* **1993**, *140*, L27.

